Infrared and Computational Studies of Spontaneously Adsorbed Amine Reagents on $YBa_2Cu_3O_7$: Structural Characterization of Monolayers atop Anisotropic Superconductor Surfaces

Jason E. Ritchie,[†] Cyndi A. Wells,[†] Ji-Ping Zhou,[†] Jianai Zhao,[†] John T. McDevitt,*[,†] Carl R. Ankrum,[‡] Luckner Jean,[‡] and David R. Kanis*[,‡]

Contribution from the Department of Chemistry and Biochemistry, The University of Texas at Austin, Austin, Texas 78712, and Department of Chemistry and Physics, Chicago State University, Chicago, Illinois 60628

Received March 4, 1997

Abstract: Methods capable of forming highly organized monolayers on top of $YBa_2Cu_3O_7$ (YBCO), a high-T_c superconductor, have been identified and are described for the first time. Here, grazing reflectance infrared fourier transform spectroscopy (GRIFTS) is employed to evaluate the degree of order for these monolayer structures. Through these investigations, it is found that while octadecylamine forms a well-ordered, crystalline-like monolayer on the surface of *c*-axis-oriented $YBa_2Cu_3O_7$ thin films, the same reagent adsorbed onto polycrystalline $YBa_2Cu_3O_7$ pellets affords disordered, liquid-like monolayers. Computational studies of alkylamine packing, using a molecular mechanics methodology, reveal two plausible structures for the crystalline-like monolayer. A GRIFTS comparison of primary, secondary, and tertiary alkylamine reagents also has been completed, and the substitution pattern dependence of the monolayer order has been assessed experimentally. Moreover, comparisons between amine monolayers on top of $YBa_2Cu_3O_7$ and alkyl thiol reagents on gold surfaces are made using GRIFTS and thermal desorption experiments. This work documents the initial report of the assembly and characterization of organized monolayers supported on high-T_c superconductor surfaces, the most complex substrate yet reported capable of fostering ordered adsorbate layers.

Introduction

Since the discovery of high-temperature superconductivity over a decade ago,[1,2] there has been a tremendous amount of excitement in the scientific and industrial communities in anticipation of the practical utilization of these remarkable materials. Unfortunately, the cuprate compounds are plagued by a number of parasitic chemical degradation reactions such as water reactivity, oxygen loss, and oxide ion electromigration. These degradation pathways have drastically slowed progress in the area of high-T_c research and product development.[3−6] Many of the envisioned technological applications and fundamental studies involving high-T_c systems rely on a firm understanding of the interfacial properties of these cuprate compounds. While initial applications using high-T_c materials approach the market place in the form of NMR pick-up coils, microwave devices, and SQUID sensors,[7−12] the true potential of this area cannot be realized until new processing methods are identified that are capable of controlling the interfacial properties of these reactive high-T_c systems.[13] To date, variations in the local chemical structure of high-T_c thin film structures have made it impossible to prepare large arrays of high-T_c junctions suitable for digital applications.[14] While the advantages of intrinsic speed and power dissipation are clearly recognized for superconductor devices relative to their semiconducting counterparts, the high-T_c digital revolution awaits further developments in areas related to the chemical processing of high-T_c systems. Clearly, the development of reliable procedures to control the local structure and interfacial properties of high-T_c materials will have an important influence on the area of high-T_c superconductivity.

Of the four classes of electronic materials (insulators,

* Author to whom correspondence should be addressed (email mcdevitt@huckel.cm.utexas.edu).

[†] The University of Texas at Austin.

[‡] Chicago State University.

(1) Kresin, V. Z.; Wolf, S. A. *Fundamentals of Superconductivity*; Plenum Press: New York, 1990.

(2) Poole, C. P.; Farach, H. A.; Creswick, R. J. *Superconductivity*; Academic Press: San Diego, CA, 1995.

(3) Zhou, J.-P.; Savoy, S. M.; Zhao, J.; Riley, D. R.; Zhu, Y. T.; Manthiram, A.; Lo, R.-K.; Borich, D.; McDevitt, J. T. *J. Am. Chem. Soc.* **1994**, *116*, 9389−9390.

(4) McDevitt, J. T.; Riley, D. R.; Haupt, S. G. *Anal. Chem.* **1993**, *65*, 535A−545A.

(5) McDevitt, J. T.; Haupt, S. G.; Jones, C. E. In *Electrochemistry of High-T_c Superconductors*; McDevitt, J. T., Haupt, S. G., Jones, C. E., Eds.; Marcel Dekker: New York, 1996; Vol. 19, pp 355−481.

(6) McDevitt, J. T.; Haupt, S. G.; Clevenger, M. B. In *Conductive Polymer/High-Temperature Superconductor Assemblies and Devices*; McDevitt, J. T., Haupt, S. G., Clevenger, M. B., Eds.; Marcel Dekker: New York, 1996; pp 1029−1058.

(7) Berkowitz, S. J.; Zhang, Y. M.; Mallison, W. H.; Char, K.; Terzioglu, E.; Beasley, M. R. *Appl. Phys. Lett.* **1996**, *69*, 3257−3259.

(8) Berkowitz, S. J.; Hirahara, A. S.; Char, K.; Grossman, E. N. *Appl. Phys. Lett.* **1996**, *69*, 2125−2127.

(9) Katz, A. S.; Sun, A. G.; Dynes, R. C.; Char, K. *Appl. Phys. Lett.* **1995**, *66*, 105−107.

(10) Koelle, D.; Miklich, A. H.; Dantsker, E.; Ludwig, F.; Nemeth, D. T.; Clarke, J.; Ruby, W.; Char, K. *Appl. Phys. Lett.* **1993**, *63*, 3630−3632.

(11) Mallison, W. H.; Berkowitz, S. J.; Hirahara, A. S.; Neal, M. J.; Char, K. *Appl. Phys. Lett.* **1996**, *68*, 3808−3810.

(12) Martens, J. S.; Pance, A.; Char, K.; Lee, L.; Whiteley, S.; Hietala, V. M. *Appl. Phys. Lett.* **1993**, *63*, 1681−1683.

(13) McDevitt, J. T.; Lo, R.-K.; Zhou, J.; Haupt, S. G.; Zhao, J.; Jurbergs, D. C.; Chen, K.; Mirkin, C. A. *Chem. Mater.* **1996**, *8*, 811−813.

(14) Talvacchio, J.; Forrester, M. G.; Hunt, B. D.; McCambridge, J. D., M.; Young, R. M.; Zhang, X. F.; Miller, J. D. *IEEE Trans. Appl. Supercond.* **1997**, *7*, 2051−2056

S0002-7863(97)00692-6 CCC: $15.00
Published on Web 03/13/1998

semiconductors, metals, and superconductors), methods for surface modification of these systems have been extensively studied in all cases except for superconductors.[15] For example, the spontaneous adsorption of monolayer films has been demonstrated for a large number of adsorbate molecules with varying functional groups; selected examples include: alkyl thiols,[16] dialkyl disulfides,[17,18] and dialkyl sulfides,[19] on Au (111), carboxylic acids on metal oxides,[20,21] trichloro- and trialkoxysilanes on oxide surfaces,[22−26] thiols on GaAs,[27] CdSe, CdS, Cu,[28,29] and Ag,[28,30] and thiols, olefins, alcohols, amines, and isonitriles on Pt.[19,31−33] Importantly, spontaneously adsorbed monolayer films have been used to examine fundamental processes involving interfacial electron transfer, adhesion, and surface wetting.[15,34] Furthermore, a variety of interesting practical applications for the adsorbed monolayers have been reported in areas such as microcontact printing,[35,36] chemical sensing,[37] corrosion protection,[29,38] nonlinear optical materials,[39] organization of nanoscale particles,[40] and high-density memory devices.[41]

Like superconductivity, the field of self-assembled monolayers (SAMs) has attracted a significant amount of attention over the past decade. Currently, the number of highly organized monolayer systems are limited to alkylsiloxanes on SiO_2, *n*-alkanoic acids on oxidized silver and aluminum, dialkyl disulfides, dialkyl sulfides, alkyl thiols on gold, and alkyl thiols on pristine silver, copper, and GaAs.[27] To date, there is no literature precedent for organized monolayers supported on anisotropic conductors and none on systems containing more than one metal binding site.[5]

Recently, we described the first effective method capable of adsorbing persistent monolayer structures onto the high-T_c superconductors: $YBa_2Cu_3O_7$, $Y_{0.6}Ca_{0.4}Ba_{1.6}La_{0.4}Cu_3O_7$ (TX-YBCO), and $Tl_{1.4}Ba_2CaCu_2O_7$.[42,43] Here, molecular reagents possessing reactive functional groups were tagged with redox-active ferrocene reagents to electrochemically assay which reagents spontaneously adsorb to the high-T_c materials. Alkylamines, arylamines, alkyl thiol, alkyl disulfides, and alkyl selenols were shown to adsorb and form stable and electroactive superconductor-localized monolayers.[42,43] Primary *n*-alkylamines were found to form to the most rugged and persistent monolayers. Electrochemically assayed surface coverages (corrected for surface roughness values), scan rate dependence of voltammetric current, contact angle, and X-ray photoelectron spectroscopy measurements together yield convincing evidence for the presence of the superconductor-localized monolayer structures. Importantly, very little change is noticed in the superconductor's electrical properties following the adsorption of the monolayer reagents. Furthermore, adsorbed electroactive monolayers display voltammetry consistent with a surface-localized monolayer (i.e., small ΔE_p values and approximately equal current for the anodic and cathodic waves). All of these factors point to the conclusion that the amine monolayer adsorption occurs through "soft chemistry", causing little damage to the fragile high-T_c substrate.

While recent reports have described the use of alkylamine, arylamine, and alkyl thiol species for the formation of persistent monolayers atop a variety of cuprate phases,[42−45] the degree of order for such superconductor-localized monolayers has yet to be reported. Indeed, comparisons with other metal oxide systems such as Al_2O_3 and SiO_2 might suggest that ordered monolayers anchored atop the complex, reactive, and anisotropic high-T_c superconductors would be difficult to obtain.[20] Indeed, for the creation of effective corrosion barriers,[13] tunnel junctions,[46] adhesion layers,[13] and molecular spacer layers for energy transfer studies, it is essential that procedures be identified that are capable of producing organized superconductor-localized monolayers.

The method of grazing reflectance infrared fourier transform spectroscopy (GRIFTS) has been used by many researchers to acquire useful qualitative and quantitative information related to the order of spontaneously adsorbed monolayers.[16,18,20,28,31,47−49] The peaks in the C−H stretching region are particularly diagnostic for the degree of crystallinity of the adsorbed monolayer. Specific frequencies and peak intensities of the various C−H vibrations yield useful information regarding the local chemical environment within the SAM layer. For the case of highly ordered, long-chain alkyl thiol monolayers on gold

(15) Ulman, A. *An Introduction to Ultrathin Organic Films, From Langmuir−Blodgett to Self-Assembly*; Academic Press: Boston, MA, 1991.
(16) Porter, M. D.; Bright, T. B.; Allara, D. L.; Chidsey, C. E. D. *J. Am. Chem. Soc.* **1987**, *109*, 3559−3568.
(17) Nuzzo, R. G.; Allara, D. L. *J. Am. Chem. Soc.* **1983**, *105*, 4481−4483.
(18) Nuzzo, R. G.; Fusco, F. A.; Allara, D. L. *J. Am. Chem. Soc.* **1987**, *109*, 2358−2368.
(19) Troughton, E. B.; Bain, C. D.; Whitesides, G. M.; Nuzzo, R. G.; Allara, D. L.; Porter, M. D. *Langmuir* **1988**, *4*, 365.
(20) Allara, D. L.; Nuzzo, R. G. *Langmuir* **1985**, *1*, 52−66.
(21) Schlotter, N. E.; Porter, M. D.; Bright, T. B.; Allara, D. L. *Chem. Phys. Lett.* **1986**, *132*, 93−98.
(22) Tripp, C. P.; Hair, M. L. *Langmuir* **1992**, *8*, 1120−1126.
(23) Parikh, A. N.; Allara, D. L.; Azouz, I. B.; Rondelez, F. *J. Phys. Chem.* **1994**, *98*, 7577−7590.
(24) Kessel, C. L.; Granick, S. *Langmuir* **1991**, *7*, 532−538.
(25) Savig, J. *J. Am. Chem. Soc.* **1980**, *102*, 92.
(26) Moaz, R.; Sagiv, J. *J. Colloid Interface Sci.* **1984**, *100*, 465−496.
(27) Sheen, C. W.; Shi, J.-X.; Martensson, J.; Parikh, A. N.; Allara, D. L. *J. Am. Chem. Soc.* **1992**, *114*, 1514−1515.
(28) Laibinis, P. E.; Whitesides, G. M.; Allara, D. L.; Tao, Y. T.; Parikh, A. N.; Nuzzo, R. G. *J. Am. Chem. Soc.* **1991**, *113*, 7152−67.
(29) Laibinis, P. E.; Whitesides, G. M. *J. Am. Chem. Soc.* **1992**, *114*, 9022−9028.
(30) Walczak, M. M.; Chung, C.; Stole, S. M.; Widrig, C. A.; Porter, M. D. *J. Am. Chem. Soc.* **1991**, *113*, 2370−2378.
(31) Hickman, J. J.; Laibinis, P. E.; Auerbach, D. I.; Zou, C.; Gardner, T. J.; Whitesides, G. M.; Wrighton, M. S. *Langmuir* **1992**, *8*, 357−359.
(32) Stern, D. A.; Laguren-Davidson, L.; Frank, D. G.; Gui, J. Y.; Lin, C.-H.; Lu, F.; Salaita, G. N.; Walton, N.; Zapien, D. C.; Hubbard, A. T. *J. Am. Chem. Soc.* **1989**, *111*, 877−891.
(33) Mebrahtu, T.; Berry, G. M.; Bravo, B. G.; Michelhaugh, S. L.; Soriaga, M. P. *Langmuir* **1988**, *4*, 1147−1151.
(34) Bard, A. J.; Abruna, H. D.; Chidsey, C. E. D.; Faulkner, L. R.; Feldberg, S. W.; Itaya, K.; Majda, M.; Melroy, O.; Murray, R. M.; Porter, M. D.; Soriaga, M. D.; White, H. S. *J. Phys. Chem.* **1993**, *97*, 7147−7173.
(35) Kumar, A.; Whitesides, G. M. *Science* **1994**, *263*, 60−62.
(36) Xia, Y.; Mrksich, M.; Kim, E.; Whitesides, G. M. *J. Am. Chem. Soc.* **1995**, *117*, 9576−9577.
(37) Dermody, D. L.; Crooks, R. M.; Kim, T. *J. Am. Chem. Soc.* **1996**, *118*, 11912−11917.
(38) Feng, Y.; Teo, W.-K.; Siow, K.-S.; Gao, Z.; Tan, K.-L.; Hsieh, A.-K. *J. Electrochem. Soc.* **1997**, *144*, 55−64.
(39) Lin, W.; Lee, T.-L.; Lyman, P. F.; Lee, J.; Bedzyk, M. J.; Marks, T. J. *J. Am. Chem. Soc.* **1997**, *119*, 2205−2211.
(40) Freeman, R. G.; Grabar, K. C.; Allison, K. J.; Bright, R. M.; Davis, J. A.; Guthrie, A. P.; Hommer, M. B.; Jackson, M. A.; Smith, P. C.; Walter, D. G.; Natan, M. J. *Science* **1995**, *267*, 1629−1632.
(41) Kawanishi, Y.; Tamaki, T.; Sakuragi, M.; Seki, T.; Suzuki, Y.; Ichimura, K. *Langmuir* **1992**, *8*, 2601.
(42) Chen, K.; Mirkin, C. A.; Lo, R.-K.; Zhao, J.; McDevitt, J. T. *J. Am. Chem. Soc.* **1995**, *117*, 1121−1122.
(43) Chen, K.; Xu, F.; Mirkin, C. A.; Lo, R.-K.; Nanjundaswamy, K. S.; Zhou, J.-P.; McDevitt, J. T. *Langmuir* **1996**, *12*, 2622−2624.
(44) Lo, R.-K.; Ritchie, J. E.; Zhou, J.-P.; Zhao, J.; McDevitt, J. T. *J. Am. Chem. Soc.* **1996**, *118*, 11295−11296.
(45) Zhu, J.; Xu, F.; Schofer, S. J.; Mirkin, C. A. *J. Am. Chem. Soc.* **1997**, *119*, 235−236.
(46) Clevenger, M. B.; Zhao, J.; McDevitt, J. T. *Chem. Mater.* **1996**, *8*, 2693−2696. Covington, M.; Xu, F.; Mirkin, C. A.; Feldman, W. L.; Greene, L. H. *Czech. J. Phys.* **1996**, *46*, 1341.
(47) Camillone, N. I.; Chidsey, C. E. D.; Liu, G.-y.; Scoles, G. *J. Chem. Phys.* **1993**, *98*, 4234−4245.
(48) Chidsey, C. E. D.; Loiacono, D. N. *Langmuir* **1990**, *6*, 682−691.
(49) Porter, M. D. *Anal. Chem.* **1988**, *60*, 1143A−1155A.

(111) surfaces, the observed frequencies for d^- (asymmetric (asym) CH_2) of 2917 cm^{-1} and d^+ (symmetric (sym) CH_2) of 2850 cm^{-1} agree well with those observed for crystalline alkanes. In addition, these results correspond well with the vibrational features observed at 2918 and 2851 cm^{-1}, which are associated with solid samples of $CH_3(CH_2)_{21}SH$ in KBr.[16] Liquid alkyl thiol samples are shown to exhibit methylene stretches at 2924 and 2855 cm^{-1}. These observations suggest that spontaneously adsorbed alkyl thiol monolayers atop gold (111) possess an extended linear structure containing very few gauche defects. Moreover, the intensities of the various $-CH_2$ and $-CH_3$ vibrations deviate markedly from those observed for the isotropic samples. From an analysis of the IR data using the transition dipole orientation with respect to the polarization vector, an estimate for the monolayer tilt angle of 20−35° has been made.[16,18,50] The calculated angle, based on the IR analysis, agrees well with data obtained from other experimental methods such as ellipsometry, He diffraction, and electron diffraction.[16,48,50,51]

While ordered monolayers have been shown to form on surfaces such as noble metal single crystals and evaporated films of metals (Ag,[21,28] Cu,[28] Au,[16,18,28] Pt), disordered monolayers are observed to form on the more complex substrates such as Al_2O_3, Al with a native oxide surface, Ag_2O, and SiO_2.[20,52] In the highly studied case of siloxane monolayers on SiO_2 surfaces, it has been found that there is a critical adsorption temperature at which the surface energy is minimized. Below this critical temperature, monolayers of octadecyltrichlorosilane with d^- (asym CH_2) values of 2917 cm^{-1} and d^+ (sym CH_2) of 2849 cm^{-1} are obtained.[23] Above this critical temperature, the methylene stretches increase in frequency, indicating that the monolayer is being deposited in a disordered manner.

A recent report describing the use of gold colloids in the context of a surface enhanced raman spectroscopy (SERS) study has yielded direct spectroscopic evidence for the association of the amine functional group with the high-T_c cuprate lattice. Using a strategy developed my Natan,[40] Mirkin and co-workers[45] have confirmed prior indirect evidence for the existence of a strong amine headgroup interaction.[13,42−44,46] Unfortunately, the 4-aminopyridine reagent (used for this study because of its high Raman cross-section) does not provide structural features analogous to hydrocarbon species commonly used to generate adsorbate monolayers and no information was reported related to its ordering characteristics.

While many metal oxide surfaces have been successfully modified with alkylsiloxane or alkylcarboxlyic acid reagents, high-T_c superconductors represent a more complex system than those previously examined. Most of the previously studied systems have had the advantage of supporting hydrated surfaces, which could then be modified with siloxane type reagents. Unfortunately, $YBa_2Cu_3O_7$ is very susceptible to corrosion by water and acids.[4,5,53−56] When exposed to the atmosphere, $YBa_2Cu_3O_7$ rapidly reacts to form nonsuperconductive corrosion products such as $BaCO_3$, Y_2BaCuO_5, and CuO.[57]

Indeed, there are several differences that set $YBa_2Cu_3O_7$ apart from prior metal oxides shown to support adsorbate monolayers. These differences include the following: (1) $YBa_2Cu_3O_7$ has a water reactive surface which is readily corroded, (2) $YBa_2Cu_3O_7$ possesses a complex and anisotropic structure composed of CuO, BaO, CuO_2, and Y 2-dimensional layers, (3) the adsorption chemistry at $YBa_2Cu_3O_7$ is complicated by the fact that the lattice is composed of three cations (Y^{3+}, Ba^{2+}, Cu^{n+}), (4) the intrinsically poor reflectivity exhibited by $YBa_2Cu_3O_7$ makes classical reflectance IR structural analysis difficult. Thus, the surface modification of $YBa_2Cu_3O_7$ does not simply represent the modification of a new metal oxide surface, but a fundamentally new class of electronic materials which presents its own set of new challenges.

There are several issues related to the structure of monolayers spontaneously adsorbed to high-T_c materials that remain unaddressed at this juncture. Important questions yet to be answered include the following: (1) Can organized monolayers be created atop real samples of anisotropic cuprate superconductors? (2) Does the sample type (i.e., ceramic vs oriented thin film) influence the degree of monolayer order? (3) Can monolayers be adsorbed onto the different crystallographic faces of $YBa_2Cu_3O_7$ [i.e., (001) vs (100) orientation]? (4) What are the structural features of these self-assembled monolayer structures, and can these be systematically altered by tailoring the substrate? (5) Can the monolayers be thermally desorbed without damage to the high-T_c lattice? (6) What role does etching play in the establishment of monolayer structures? (7) How are the superconductor properties influenced by the monolayer adsorption process?

In this paper, the GRIFTS method is used to explore the degree of ordering of amine monolayers on $YBa_2Cu_3O_7$ samples. Both polycrystalline ceramic samples as well as (001) and (100) oriented thin films are examined in this context. Moreover, the studies are extended to an analysis of the ordering properties for primary, secondary, and tertiary amine reagents. Using the IR data combined with computational studies, plausible structures for selected monolayers are proposed and discussed.

Experimental Section

Sample Preparation and Treatment. Gold film samples were deposited as 2000 Å thick layers, prepared by resistive evaporation (Edwards Auto 306 Metal Evaporator equipped with cryodrive pump) onto a 50 Å Cr adhesion layer. Film thickness values were monitored with an in-situ quartz crystal microbalance. Silicon and glass substrates were used to support the metal layers. Both of these substrates were cleaned with pihrana solution, H_2O_2/H_2SO_4 (1:3) (*CAUTION! extremely corrosive*), immediately prior to deposition. Evaporated gold samples were used soon after their evaporation. Gold evaporated onto glass and silicon substrates were examined by X-ray powder diffraction. These gold samples exhibited only the (111) diffraction peak indicating a >95% (111) orientation. On the other hand, gold samples evaporated onto $YBa_2Cu_3O_7$ pellets were shown to yield a relatively strong (002) diffraction peak in addition to the (111) reflection, indicating the presence of alternative orientations in these films. From these experiments, it is clear that polycrystalline gold films are prepared when the metal is deposited atop the polycrystalline cuprate surface.

Ceramic pellets of $YBa_2Cu_3O_7$ were prepared by standard solid-state synthesis methods.[58] Here, Y_2O_3, CuO, and $BaCO_3$ were combined and ground for 45 min using an agate mortar and pestle. The resulting gray mixture was then placed into an alumina crucible and fired for 24 h at 900 °C in a box-type furnace. The resulting black powder was

(50) Strong, L.; Whitesides, G. M. *Langmuir* **1988**, *4*, 546−558.
(51) Nuzzo, R. G.; Dubois, L. H.; Allara, D. L. *J. Am. Chem. Soc.* **1990**, *112*, 558−569.
(52) Golden, W. G.; Snyder, C. D.; Smith, B. *J. Phys. Chem.* **1982**, *86*, 4675−4678.
(53) Zhou, J.-P.; Lo, R.-K.; Savoy, S. M.; Arendt, M.; Armstrong, J.; Yang, D.-Y.; Talvacchio, J.; McDevitt, J. T. *Phys. C* **1997**, *273*, 223−232.
(54) Riley, D. R.; Jurbergs, D. J.; Zhou, J.-P.; Zhao, J.; Markert, J. T.; McDevitt, J. T. *Solid State Commun.* **1993**, *88*, 431−434.
(55) Riley, D. R.; McDevitt, J. T. *J. Electroanal. Chem.* **1990**, *295*, 373−384.
(56) Zhou, J.-P.; McDevitt, J. T. *Chem. Mater.* **1992**, *4*, 953−959.
(57) Barkatt, A.; Hojaji, H.; Amarakoon, V. R. W.; Fagan, J. G. *MRS Bull.* **1993**, *18*, 45−52.
(58) Schneemeyer, L. F. In *Crystal Growth and Solid State Synthesis of Oxide Superconductors*; Schneemeyer, L. F., Ed.; Noyes: Park Ridge, NJ, 1992.

then reground for 45 min, pressed into 1 cm diameter pellets, and sintered for 24 h at 900 °C. These pellets were then broken up in a porcelain mortar and ground for the final time into a very loose powder. The $YBa_2Cu_3O_7$ powder was repressed into a 2.5 cm diameter pellets (5 g of $YBa_2Cu_3O_7$) and fired for 24 h at 900 °C. These pellets were then annealed in a tube furnace at 550 °C under flowing oxygen for 12 h. The use of large pellets is necessary to maximize the signal from the infrared measurement (*vide infra*).

Thin films of both (001) and (100) oriented $YBa_2Cu_3O_7$ were prepared by the pulsed laser ablation method.[59] Here, a $YBa_2Cu_3O_7$ ceramic target was mounted in a deposition chamber which was evacuated to a base pressure of 1×10^{-7} Torr. A KrF excimer laser beam (248 nm, 20 ns pulse width) was focused onto the target at an angle of 45° to produce a 2 J cm^{-2} energy density on the surface of the target. The substrates (typically $LaAlO_3$ single crystals) were mounted 5 cm from the target. The resulting crystallographic orientation of $YBa_2Cu_3O_7$ thin films are dependent on the substrate temperature used during the pulsed laser ablation. To prepare a (001) oriented thin film, a substrate temperature of 760 °C is maintained during the deposition, while a (100) oriented film is obtained when a substrate temperature of 680 °C is used. Optimal results were obtained when a deposition rate of 1 Å per pulse, and a 100 mTorr oxygen partial pressure were used. After deposition the samples were cooled to 450 °C where they were maintained for approximately 20 min in a 1 Torr oxygen atmosphere. The film samples were then cooled to room temperature in the same oxygen atmosphere.

The thin film superconductor samples were fully characterized by X-ray powder diffraction and four probe conductivity measurements. All superconductor specimens used in these experiments showed metallic temperature dependence of resistivity, and a superconducting critical temperature of 90 K. The (001) oriented film samples were shown by X-ray diffraction to exhibit nearly exclusive *c*-axis orientation, while the (100) oriented films were shown to contain 95% (100) oriented material. The $YBa_2Cu_3O_7$ thin films used in these experiments were 3000 Å in thickness and were supported on single-crystal $LaAlO_3$ (100) substrates (2 cm × 2 cm × 1 mm). It was necessary to use the large films to maximize the signal from the infrared measurement, as well as achieving reproducible sample alignment.

Monolayer adsorption experiments were carried out by soaking the substrates in a 1 mM solution of the adsorbate molecule in hexanes. Typically, samples were allowed to remain in the solution for 18−24 h. Upon removal from the adsorption bath, substrates were sequentially washed by immersion in four baths of hexanes to remove any physisorbed amine reagent. After the final washing step, samples were blown dry in a stream of dry nitrogen. Film specimens were immediately characterized by infrared measurements.

Infrared Measurements. Grazing reflectance infrared fourier transform spectra (GRIFTS) were acquired on a Nicolet 550 Fourier-transform spectrometer equipped with a liquid nitrogen cooled mercury−cadmium−telluride (MCT) detector. This spectrometer was adapted with a spectral reflectance attachment, which was aligned so that radiation was delivered to the sample at an angle of 79° to the surface normal for the majority of the experiments.[60] In selected cases, alternative incident angles were employed resulting in qualitatively similar spectral features. No attempt is made here to utilize measured absorbance values along with dipole analysis to estimate tilt angles as per previously described method of Allara and Nuzzo.[20] Before such measurements are possible, complete characterization of the optical constants of $YBa_2Cu_3O_7$ is necessary. Complications related to reactivity properties of the cuprate compound presently preclude an accurate and reliable analysis of this type. Future detailed studies may overcome this limitation. The incident radiation was polarized perpendicular to the plane of the substrate (i.e., p-polarized). Spectra were acquired at 4 cm^{-1} resolution with a mirror speed of 1.4 cm/s. Typically, 4000 scans were obtained so as to achieve a spectrum with an adequate signal-to-noise ratio. Background spectra were acquired on the substrate immediately after deposition and prior to adsorption of the monolayer reagent. Atmospheric exposure of the film samples was minimized.

Transmission FT-IR spectra were acquired for selected samples using a second Nicolet 550 spectrometer that was equipped with a deuterated triglycerine sulfate (DTGS) pyroelectric detector. Spectra of liquid samples were acquired using drops of the liquid confined between KBr salt plates, whereas solid samples were incorporated into pressed KBr pellets.

Computational Studies. All molecular mechanics computations reported in this work employed an MM2 force field with standard MM2 parameters.[61−63] Specifically, the Molecular Mechanics algorithm in the CAChe (Computer-Aided Chemistry) package was used with default parameters specified. The rigid molecule chosen for the majority of the studies was an energy-minimized geometry of a five-carbon primary amine ($NH_2(CH_2)_4CH_3$). The geometry of the prototype amine was optimized at an ab initio level (6-311G** basis set) using the Mulliken algorithm in the CAChe software package.[64] The free energy of each monolayer assembly was explored by comparing two different geometries of monolayers. The first geometry was composed of four duplicate amines placed over a 3 × 3 copper lattice, aligned in one plane and spatially separated from one another by a distance corresponding to the $\sqrt{2}\times\sqrt{2}$R45° adlayer separation of (001) oriented $YBa_2Cu_3O_7$, with the chains occupying the four corner adsorption sites. Note that the middle copper site is left vacant in this geometry. The second geometry was identical to the first except that the previously vacant middle copper site is occupied by a fifth chain. These geometries are schematically illustrated in Figure 8. This technique minimizes artificial variations in the computed energies due to edge effects. In addition, studies of alkyl thiol reagents adsorbed on to gold (111) surfaces were completed to determine the reliability of the described computational studies. Energy terms related to the lattice and the headgroup−substrate interaction were not evaluated in this study.

Plausible structures were identified on the basis of the minimized intermolecular energy between the amines in the various test sets. Within the framework of molecular mechanics, the total potential energy of a system can be partitioned into bond stretches, angle bends, torsion bends, van der Waals' interactions, and electrostatic interactions. The last two terms are the intermolecular contributions to the potential energy. Because van der Waals' forces were cut off at 9 Å in our model, the energy differences between the four- and five-chain systems were determined primarily by interaction of the center chain with its nearest neighbors. These van der Waals' 6−12 terms dominate the electrostatic terms in the molecule−molecule potential energy of our system.

To ensure that the MM2 computations were providing reliable results, we also carried out PM3 computations on a representative series of orientations. All PM3 computations were performed using the MOPAC algorithm in the CAChe software package, with none of the semi-empirical parameters modified.[65,66] The ab initio and MOPAC computations were carried out on an Apple Work Group 500 Server (256 MB of RAM) using CAChe for Workgroups,[63] whereas the mechanics computations were carried out using the Personal CAChe software on a Power Macintosh.[67]

Molecular Reagents. Octadecylamine, trioctylamine, and dioctylamine compounds were obtained as reagent grade from Aldrich and were used as received. Reagent grade hexanes was used as received. High-T_c starting materials, yttria, barium carbonate, and copper oxide were purchased from Alfa Aesar, all as high purity (99.99%) compounds.

(59) Miyazawa, S.; Tazoh, Y.; Asano, H.; Nagai, Y.; Michikami, O. *Adv. Mater.* **1993**, *5*, 179.
(60) Finklea, H. O.; Melendez, J. A. *Spectroscopy* **1986**, *1*, 47−48.
(61) Allinger, N. L. *J. Am. Chem. Soc.* **1977**, *99*, 8127−8134.
(62) Berkert, U.; Allinger, N. L. *Molecular Mechanics*; American Chemical Society: Washington, DC, 1982.
(63) Clark, T. *A Handbook of Computational Chemistry*; Wiley: New York, 1985.
(64) CACheIBM, Oxford Molecular/IBM, CAChe Workgroup Software Package containing Mulliken Version 3.7.2, Beaverton, Oregon.
(65) Stewart, J. J. P. *J. Comput. Chem.* **1989**, *10*, 209−220.
(66) Dewar, M. J. S.; Thiel, W. I. *J. Am. Chem. Soc.* **1977**, *99*, 4899−4907.
(67) CACheMOPAC, Oxford Molecular, Personal CAChe Software Package containing MOPAC Version 6.0, Beaverton, Oregon.

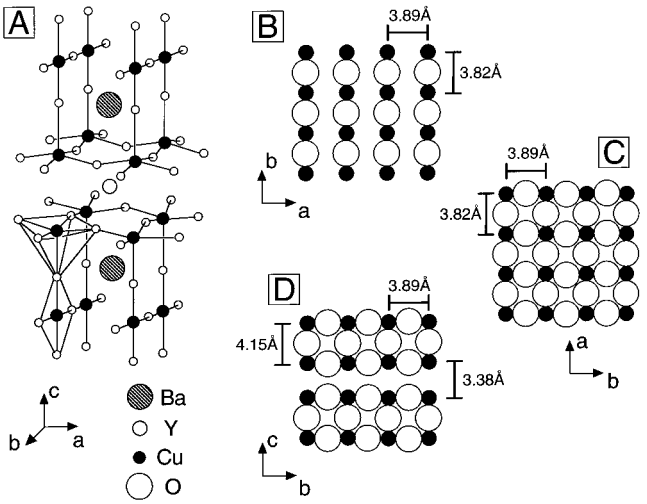

Figure 1. The unit cell of $YBa_2Cu_3O_7$ and the copper-containing layers are illustrated. Shown in (A) is the unit cell of $YBa_2Cu_3O_7$, in (B) the structure of the copper chain layer of (001) oriented $YBa_2Cu_3O_7$, in (C) the copper sheet layer of (001) oriented $YBa_2Cu_3O_7$, and in (D) the expected copper containing termination for a (100) oriented $YBa_2Cu_3O_7$ sample.

Results and Discussion

The high-T_c superconductor, $YBa_2Cu_3O_7$, was chosen for the monolayer adsorption studies for a number of reasons. First, the material can be prepared easily as a single phase both in ceramic (i.e., polycrystalline) and thin film form. Moreover, the compound represents one of the most technologically and scientifically important high-T_c phases, making its use in monolayer adsorption chemistry particularly relevant.

The compound, $YBa_2Cu_3O_7$, possesses a number of interesting and important structural features that are highlighted in Figure 1. The lattice of $YBa_2Cu_3O_7$ is composed of six sheets which are stacked along the *c*-axis in the order of Cu(1)O, BaO, $Cu(2)O_2$, Y, Cu(2)O, and BaO (Figure 1A). In principle, any of the metal cations could support the adsorption of the amine reagents. However, there are a number of factors which support the presumption that amines adsorb only at copper sites. First, copper/amine coordination chemistry is more prevalent than for any of the other metal cations present in the lattice.[68] Second, prior studies by Ellis and co-workers have documented copper cations leaching away from the high-T_c lattice upon its exposure to high concentrations of chelating amine reagents.[69] We have also obtained UV−vis and atomic adsorption spectral data consistent with copper/amine complexes when high-T_c samples have been soaked in amine reagents (i.e., hexylamine) for extended periods of time.

Monolayer adsorption onto $YBa_2Cu_3O_7$ surfaces has a large dependence on the type of sample onto which the molecule is adsorbed. Here, both polycrystalline and various thin film structures are considered (Figure S1, Supporting Information). Polycrystalline $YBa_2Cu_3O_7$ is composed of individual grains, 2−10 μm in size, which are fused together as a sintered ceramic pellet to create a sample having good mechanical integrity. Very little long-range crystallographic order is seen in such specimens.

Deposition of $YBa_2Cu_3O_7$ thin films onto a variety of single-crystal substrates allows for the creation of oriented and ordered superconductor samples. Matching between the superconductor lattice parameters and those of the substrate allow for the preparation of $YBa_2Cu_3O_7$ samples having both (001) and (100) orientations. A substrate temperature of 760 °C is used here to prepare $YBa_2Cu_3O_7$ samples having (001) orientations. These samples display relatively smooth surface morphologies (*vide infra)*. Samples of this type have surfaces which expose the *a*−*b*-plane of the lattice. High-T_c films with $YBa_2Cu_3O_7$ having (100) orientations are produced by using a lower deposition temperature of 680 °C. These samples display a rougher, more textured surface (*vide infra*). The dependence of the monolayer adsorption and ordering characteristics on crystallographic surfaces can be assayed by investigating the behavior fostered by these three types of surfaces.

Most $YBa_2Cu_3O_7$ single crystals are prepared at elevated temperatures in which they are formed in a tetragonal environment.[58] Upon cooling, extra oxygen is taken up by the lattice leading to the formation of an orthorhombic material. To relieve lattice stress, twinning along the (110) plane occurs. Thus, most $YBa_2Cu_3O_7$ single crystals possess twinned microstructures which may influence the monolayer ordering characteristics. The same behavior is also prevalent for the *c*-axis-oriented high-T_c films described below.

Before alkylamine monolayers can be reliably and reproducibly adsorbed to $YBa_2Cu_3O_7$, several problems related to the complex cuprate substrate must be overcome: (1) Samples having relatively low surface roughness values must be used. Here, we employed smooth *c*-axis-oriented films of $YBa_2Cu_3O_7$ as prepared by pulsed laser ablation for the majority of our studies. (2) Surface reactivity problems must be minimized. This objective is accomplished by using the superconductor samples immediately following their deposition, and by using only rigorously dried solvents for the monolayer adsorption steps. (3) Samples of $YBa_2Cu_3O_7$ exhibit poor reflectivity values in the infrared as compared to more conventional metals such as Au, Ag, and Al.[70] To overcome this limitation, it is necessary to use high-T_c samples having large thickness values relative to the optical penetration depth. Likewise, ceramic pellets of $YBa_2Cu_3O_7$ can be evaluated when disks with 2 cm diameter and 0.5 cm thickness are used, but the quality of the resulting spectra are inferior to those obtained with films. For $YBa_2Cu_3O_7$ films, samples with thicknesses greater than 3000 Å are used to achieve adequate reflectivity properties.

Important information related to the structural properties of the superconductor-localized monolayers can be obtained through comparisons made with the thoroughly studied alkyl thiol system on gold (111), upon which well-ordered monolayers are known to form.[16,18] Thus, both alkyl thiols on gold and alkylamines on $YBa_2Cu_3O_7$ are studied here. To evaluate the contribution of surface roughness to the monolayer structure, data is also acquired for alkyl thiol monolayers on smooth gold (111) surfaces as well as for rough polycrystalline gold deposited atop ceramic $YBa_2Cu_3O_7$ pellets.

Smooth, Oriented $YBa_2Cu_3O_7$ Surfaces. Prior work on metal oxides (SiO_2, Al_2O_3) has focused mainly on the coupling of monolayers to the oxide surfaces using Si−O−R linkages. Monolayers resulting from this type of chemistry have been shown to be disordered.[20] Attempts to employ similar chemistry for high-T_c superconductors resulted in a significant amount of

(68) Cotton, F. A.; Wilkinson, G. *Advanced Inorganic Chemistry*; Wiley-Interscience: New York, 1988.

(69) James, P. M.; Thompson, E. J.; Ellis, A. B. *Chem. Mater.* **1991**, *3*, 1087−1092.

(70) A comparison of the IR reflectivity of $YBa_2Cu_3O_7$ and gold samples, recorded in the mid-IR, showed important thickness and morphology dependencies. At 1600 cm^{-1}, a 1000 Å $YBa_2Cu_3O_7$ (001) film showed a reflectivity, relative to 2500 Å gold film, of 41%. Whereas, a 2500 Å $YBa_2Cu_3O_7$ (001) film showed a relative reflectivity of 52%. Under identical conditions, a ceramic pellet of $YBa_2Cu_3O_7$ displayed a relative reflectivity of only 8%. To maximize the signal obtained from $YBa_2Cu_3O_7$ samples, it is necessary to maximize the reflectivity and the sample size.

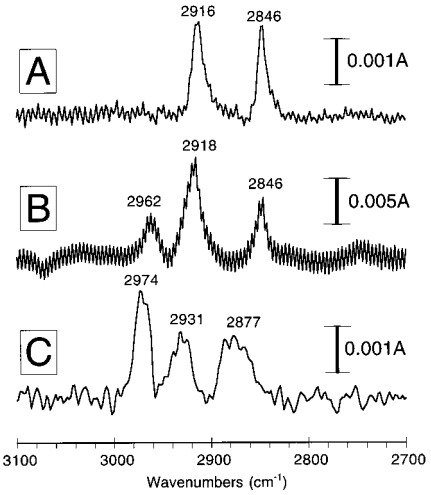

Figure 2. Shown are GRIFTS spectra obtained for octadecylamine monolayers which are supported on top of various types of $YBa_2Cu_3O_7$ surfaces: (A) a smooth (001) oriented $YBa_2Cu_3O_7$ film prepared by laser ablation, (B) a smooth (100) oriented $YBa_2Cu_3O_7$ film prepared by the same method, and (C) a polycrystalline ceramic pellet of $YBa_2Cu_3O_7$ made by a solid-state route.

damage done to the cuprate material.[71] However, octadecylamine spontaneously adsorbs to $YBa_2Cu_3O_7$ (001) films samples from a 1 mM solution in hexanes. When the resulting octadecylamine monolayer is examined by GRIFTS, two peaks are seen in the CH stretching region (Figure 2A). The frequencies of the peaks are 2916 and 2846 cm^{-1}. These peaks are assigned as the asymmetric and symmetric methylene stretching modes, respectively.

When comparing the GRIFTS spectra of octadecylamine on $YBa_2Cu_3O_7$ (001) and octadecyl thiol on gold (111), it is immediately apparent that although the methylene vibrational modes are similar in appearance, the methyl vibrations from the modified $YBa_2Cu_3O_7$ sample are conspicuously absent (Figure 2A). These infrared characteristics for octadecylamine on $YBa_2Cu_3O_7$ (001) are very reminiscent of the spectral features of alkyl thiols adsorbed to GaAs (100) acquired by Allara and co-workers.[27] The alkyl thiol/GaAs system was found to exhibit a very large molecular tilt angle of 57° from surface normal. A qualitative comparison of the GRIFTS data for the thiol/GaAs system with that observed at high-T_c adsorbate layer suggests a large tilt angle is also present for the cuprate system. This lack of methyl signal can be explained by an analysis of the vibrational dipoles (Figure S2, Supporting Information).

In addition to the position of the peaks in the GRIFTS spectra, the width of the vibrational modes can be used to diagnose the crystallinity of the hydrocarbon-based monolayer.[72] Shown in Table 1 is a compilation of peak positions and full width at half maximum (fwhm) spectral widths for all of the monolayer systems investigated in this report. The asymmetric methylene stretch of octadecylamine adsorbed to a $YBa_2Cu_3O_7$ (001) oriented thin film shows a fwhm of the asymmetric methylene stretch of 12 cm^{-1} (Table 1). Crystalline octadecyl thiol monolayers adsorbed to gold (111) surfaces show fwhm of 10 cm^{-1}, while disordered monolayers of hexadecanoic acid adsorbed to Al_2O_3 show fwhm of 34 cm^{-1}.[20] From this highly reproducible measurement, it may be inferred that octadecylamine monolayers adsorb onto $YBa_2Cu_3O_7$ (001) films in such manner that structures exhibiting a high degree of average chain-conformational order are obtained.

(71) Ritchie, J. E.; Murray, W.; McDevitt, J. T. Manuscript in preparation.
(72) Byrd, H.; Pike, J. K.; Talham, D. R. *Chem. Mater.* **1993**, *5*, 709−715.

Table 1. Comparison of the Antisymmetric Methylene Stretches for a Variety of Substrates, Monolayers, and Substitution Patterns

substrate	monolayer	frequency (cm^{-1})	fwhm (cm^{-1})
gold/silicon	$CH_3(CH_2)_{17}SH$	2917	10
gold/glass	$CH_3(CH_2)_{17}SH$	2918	9
gold/YBCO pellet	$CH_3(CH_2)_{17}SH$	2928	33
YBCO film (001)	$CH_3(CH_2)_{17}NH_2$	2916	12
YBCO film (001)	$(CH_3(CH_2)_7)_2NH$	2931	14
YBCO film (001)	$(CH_3(CH_2)_7)_3N$	2929	23
YBCO film (100)	$CH_3(CH_2)_{17}NH_2$	2918	20
YBCO pellet	$CH_3(CH_2)_{17}NH_2$	2931	22
YBCO pellet	$(CH_3(CH_2)_7)_2NH$	2929	29
YBCO pellet	$(CH_3(CH_2)_7)_3N$	2933	19
alumina[a]	$CH_3(CH_2)_{14}COOH$	2926	34
neat solid	$CH_3(CH_2)_{17}NH_2$[c]	2917	24
neat solid[a]	$CH_3(CH_2)_{14}COOH$[c]	2918	11
neat liquid[b]	$CH_3(CH_2)_7SH$[c]	2924	*d*
neat solid[b]	$CH_3(CH_2)_{21}SH$[c]	2918	*d*

[a] Adapted from Allara, D.L., et al., *Langmuir*, **1985**, *1*, 52−66 [b] Adapted from Porter, M.D., et al., *J. Am. Chem. Soc*., **1987**, *109*, 3559−3568. [c] Indicates that measurement was made in transmission mode without the use of a substrate. [d] These data were not supplied for these cases.

Shown in Figure 2B is a GRIFTS spectrum of octadecylamine adsorbed to (100) oriented $YBa_2Cu_3O_7$ film.[73] These data displays similar features seen when the same molecule is adsorbed to (001) oriented $YBa_2Cu_3O_7$, including the presence of the asymmetric methylene stretch at 2918 cm^{-1}. However, the in-plane asymmetric methyl stretch is also seen at 2962 cm^{-1} for this substrate. The reappearance of the methyl vibration may be caused by a smaller tilt angle in the adsorbate layer fostered by the presence of short Cu−Cu separations for the exposed (100) surface (*vide infra*).

While the asymmetric methylene stretch of octadecylamine adsorbed to $YBa_2Cu_3O_7$ (100) films is observed to be centered in the same place as the (001) oriented samples, the spectral width is this peak is slightly greater than that of the (001) oriented sample (20 cm^{-1} vs 8−12 cm^{-1}, see Table 1). This behavior is most likely due to the decreased order of the copper spacing in the (100) oriented film samples. Although the surface copper−copper distances in the *a* and *b* lattice directions are nearly the same for (001) oriented $YBa_2Cu_3O_7$ film (Figure 1B,C), there is a significant difference in the copper−copper spacings for (100) oriented $YBa_2Cu_3O_7$ samples (Figure 1D). This difference in spacing may lead to a decrease in the chemical homogeneity of the resulting monolayer on (100) oriented samples. While the spectral width of the asymmetric methylene stretch of the monolayer atop (100) oriented $YBa_2Cu_3O_7$ is somewhat broader than seen in other "ordered" monolayers, the positioning of the peak is good evidence that the monolayer adopts a relatively ordered structure on this substrate. Due to the width of this peak, it is probable that this structure possesses more defects than previously seen in other ordered cases.

Having identified vibrational characteristics consistent with the formation of crystalline monolayer structures,[16] it now becomes important to consider possible packing structures for the adsorbed hydrocarbon monolayers. The surface structure

(73) Note also that this sample displays periodic features that appear to be present as "background noise." However, more careful analysis of the frequency of such peaks suggests they are caused by an interference phenomenon. Likewise, the frequency dependence of these peaks/troughs corresponds exactly with constructive/destructive wave combinations reflected from exterior and interior surfaces of the high-T_c film. Roughening of the substrate with etching and thermal annealing steps reduces the magnitude of these interference fringes and can improve the appearance of the spectral features.

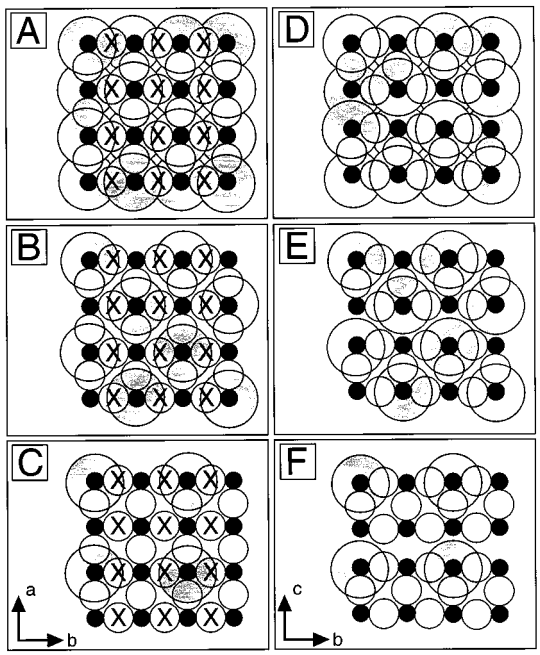

Figure 3. Possible packing structures for primary linear alkylamine monolayers on $YBa_2Cu_3O_7$. For this simplistic diagram, the footprint of the hydrocarbon is shown as a circle with dimensions corresponding to a van der Waals' radius of 4.5 Å.[16] Shown in (A) and (D) are the 1×1 monolayer adlayers for the (001) surface (A) and for the (100) oriented surface (D). Likewise, (B) and (E) show the $\sqrt{2}\times\sqrt{2}$R45° adlayer for the (001) surface (B) and the (100) oriented surface (E). Shown in (C) and (F) are the 2×2 adlayer for (001) (C) and (100) (F) oriented samples. Oxygen atoms marked with "X" indicate oxygens that are not present in the copper chain layer of the (001) oriented film but that are present in the copper sheet layer of (001) oriented $YBa_2Cu_3O_7$ films (see Figure 1).

of $YBa_2Cu_3O_7$ is somewhat complicated, having several layers that could support spontaneous adsorption of alkylamines. The unit cell of $YBa_2Cu_3O_7$ contains six distinct layers along the *c*-axis. While three of these layers do not contain copper, their presence may complicate the analysis. In (001) oriented samples of $YBa_2Cu_3O_7$, spontaneous adsorption of alkylamines is likely to occur at either the copper chain (CuO) or copper sheet (CuO_2) layer (Figure 1B,C, respectively). For (100) oriented $YBa_2Cu_3O_7$ samples, there is only one unique copper-containing layer (Figure 1D).

Shown in Figure 3 is the spatial distribution for the CuO_2 and CuO sheet layers as well as the molecular "footprint" for the hydrocarbon reagent. These diagrams illustrate the features of the docking sites for both the (001) and (100) exposed surfaces of $YBa_2Cu_3O_7$. The van der Waals' distance within paraffin crystals of 4.5 Å[16] would seem to preclude the adsorption of the amine reagents at every exposed copper site. The adsorption of alkylamines at every exposed copper site (Figure 3A) would lead to a 1×1 adlayer with a 3.8 Å separation between hydrocarbon chains; far too compact to represent a realistic packing motif. On the other hand, a $\sqrt{2}\times\sqrt{2}$R45° adlayer (Figure 3B) yields a good monolayer coverage with a headgroup separation of 5.4 Å. The adsorption of alkylamine at every other copper site without using diagonal sites leads to a 2×2 adlayer with a 7.4 Å distance separating the alkyl chains. This packing motif is probably too diffuse to promote strong chain−chain interactions (*vide infra*).

The separation achieved for the $\sqrt{2}\times\sqrt{2}$R45° case is about 10% larger than previously observed for alkyl thiol reagents on Au (111).[16] To compensate for the larger separation, an increase in the molecular tilt axis (θ_m) is expected. Molecular space filling models predict a θ_m value of 27° for alkyl thiol on gold (111),[16] which is in good agreement with experimental data. Likewise, a value of at least 35° is predicted for alkylamine monolayers on $YBa_2Cu_3O_7$ (001) (Figures S3 and S4, Supporting Information). This tilt angle prediction is based on a tilting of the monolayer chains in the (110) plane of $YBa_2Cu_3O_7$. If the monolayer chains were to be tilted in the (100) or (010) plane of the lattice, the predicted tilt angle is found to increase to 50° due to the larger copper−copper distance in the (100) and (010) lattice dimensions (Figure 1B).

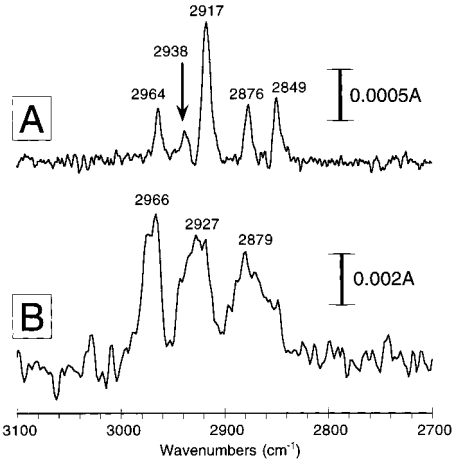

Figure 4. Shown here are GRIFTS spectra for octadecyl thiol monolayers that are adsorbed to two different gold surfaces: (A) a smooth (111) oriented gold film prepared by the evaporation onto glass and (B) a rough, polycrystalline gold surface prepared by the evaporation of gold onto a ceramic pellet of $YBa_2Cu_3O_7$.

Polycrystalline $YBa_2Cu_3O_7$ and Au Surfaces. Polycrystalline ceramic samples of $YBa_2Cu_3O_7$, when exposed to octadecylamine, are found to support the adsorption of monolayers as shown in Figure 2C. While both (100) and (001) oriented films of $YBa_2Cu_3O_7$ serve as templates for growth of ordered monolayers of the primary amine reagent, the same molecule adsorbed on ceramic surfaces is found to be highly disordered as evidenced by the asymmetric methylene stretching frequency of 2931 cm^{-1} as well the peak width of 22 cm^{-1} (Table 1).

To further explore the role of surface roughness on a more classical substrate, alkyl thiol reagents were adsorbed onto smooth and polycrystalline gold surfaces. For the former, Au (111) was evaporated onto smooth glass substrates according to standard literature procedures.[50,74] Shown in Figure 4A is a GRIFTS spectra showing the C−H stretching region for octadecyl thiol adsorbed onto an evaporated film of gold (111). This spectra replicates the five main C−H vibrational modes noted previously for this system.[16,18] Three of the modes (2964, 2938, 2876 cm^{-1}) are assigned to the CH_3 modes, and the other two modes (2917, 2849 cm^{-1}) are attributed to the CH_2 vibrations.[20]

As mentioned above, the frequencies of the alkyl modes are diagnostic of the crystallinity of the hydrocarbon-based monolayer. Spectra of octadecyl thiol adsorbed onto Au (111) show the antisymmetric methylene stretch at 2917 cm^{-1} (Figure 4A), the frequency of which corresponds nicely to solid paraffin. A crystalline-like monolayer structure is suggested from these data.[16,18]

While XRD experiments showed that gold evaporated onto glass substrates exhibited exclusive (111) orientation, gold that

(74) Willicut, R. J.; McCarley, R. L. *Langmuir* **1995**, *11*, 296−301.

is evaporated onto a rough $YBa_2Cu_3O_7$ ceramic samples adopts rough morphological characteristics and yields polycrystalline orientations. Use of this roughened gold as a substrate for monolayer adsorption allows the dependence of the substrate roughness to be studied for the well-characterized adsorbate system. Accordingly, shown in Figure 4B is a GRIFTS spectrum of octadecyl thiol adsorbed to this roughened gold system. These data shows the typical signature of a disordered monolayer, that is, the asymmetric methylene stretch appears at 2927 cm^{-1} with a spectral width of 33 cm^{-1}. These results demonstrate that there is a strong dependence on the quality (i.e., the smoothness and the orientation) of the monolayer adsorption substrate.

Poirier has extensively studied the role of substrate defects and their affect on the crystallinity of the adsorbed monolayer.[75] These prior studies concluded that small concentrations (<5%) of defects in the substrate do not affect the crystallinity of the resulting monolayer. However, substrates that have larger concentrations of defects, or are highly roughened, do not possess the long-range order necessary to produce a well-ordered monolayer film. Defects in the $YBa_2Cu_3O_7$ lattice primarily occur at the grain boundaries. While grain sizes within the films are actually smaller than those observed for the ceramic specimens, the relative orientation grain-to-grain is much more controlled for the films relative to the ceramics.

Atomic force microscopy (AFM) was used to quantify the surface roughness properties of these substrates. Using AFM, dramatic differences in the root-mean-square (RMS) roughness values were measured for evaporated gold on glass (4.39 nm), a (001) oriented $YBa_2Cu_3O_7$ thin film (17.0 nm), a (100) oriented $YBa_2Cu_3O_7$ thin film (30.9 nm), and a particularly smooth polycrystalline $YBa_2Cu_3O_7$ pellet (293 nm). In general, ceramic pellets of $YBa_2Cu_3O_7$ are much too rough to evaluate by AFM instrumentation. Shown in Figure 5 are typical AFM images of the surfaces examined in this report. Also included is a profilometry measurement of the surface of a typical polycrystalline $YBa_2Cu_3O_7$ pellet (Figure 5D). The two different $YBa_2Cu_3O_7$ samples seen in Figure 5 are of comparable roughness, whereas the gold film is significantly smoother and the ceramic pellet is significantly rougher.

From these images it is clear that oriented $YBa_2Cu_3O_7$ thin film samples are relatively smooth as are evaporated gold specimens. The surface morphological characteristics allow for the formation of compact and crystalline monolayers. The roughness of the $YBa_2Cu_3O_7$ ceramic pellet, and the gold surface that was deposited thereon, precludes any long-range order, which would be necessary for the formation of compact and crystalline monolayers. Given the results for the polycrystalline $YBa_2Cu_3O_7$ and the data from the polycrystalline gold case, a strong argument can be made that the smoothness, orientation, and defect density of the substrate are critical factors for producing compact, ordered, and defect-free monolayers.

Alkylamine Substitution Pattern Dependence. Amines offer the capability of being substituted to various degrees allowing for studies involving the substitution pattern dependence of monolayer ordering characteristics. We find that the substitution pattern of the monolayer reagent plays a vital role in the crystallinity of the resulting monolayer. While, monothiol-based reagents can accommodate only one alkyl substituent directly attached to the sulfur headgroup, amines can possess up to three alkyl substituents. Interestingly, we observe that primary (octadecylamine), secondary (dioctylamine), and tertiary amines (trioctylamine) all spontaneously adsorb to $YBa_2Cu_3O_7$.

(75) Poirier, G. E. *Langmuir* **1997**, *13*, 2019−2026.

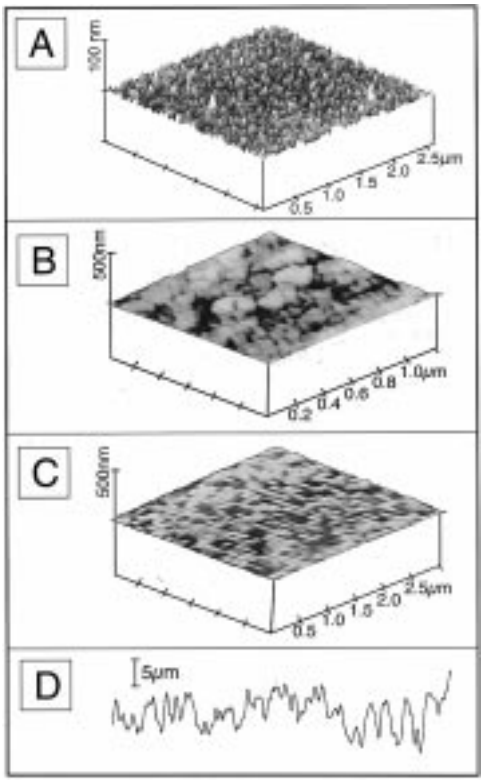

Figure 5. Shown are AFM images and a profilometry trace for the four substrates studied herein. Included here are AFM images of (A) a typical evaporated gold film, (B) a (001) oriented $YBa_2Cu_3O_7$ film, (C) a (100) oriented $YBa_2Cu_3O_7$ film, and (D) a profilometer trace of a typical polycrystalline $YBa_2Cu_3O_7$ pellet. For the last case, the length over which the profilometry trace was recorded was 2000 μm. The large *Z* range for the $YBa_2Cu_3O_7$ pellet prevented an AFM measurement on this surface.

However, the secondary and tertiary amines do not form crystalline monolayers on $YBa_2Cu_3O_7$ (001) films or pellets (Table 1) as do the above-described primary amines. Rather, the GRIFTS spectra obtained for these samples are very similar to the primary amine reagents adsorbed on rough substrates. Shown in Figure 6 is a comparison of trioctylamine, dioctylamine, and octadecylamine adsorbed to $YBa_2Cu_3O_7$ (001) oriented thin films. In addition, spectra of these same three amine reagents were taken on rough $YBa_2Cu_3O_7$ ceramic samples (not shown). These spectra are very similar to those shown in Figure 6, and the results of such studies are summarized in Table 1.

It is apparent from the peak position and peak width measurements that the secondary and tertiary amines form disordered monolayers when adsorbed to both rough and smooth substrates. This behavior indicates that the crystallinity of the resulting monolayer is strongly dependent on the substitution pattern of the amine monolayer reagent.

Thermal Desorption. The GRIFTS technique was also employed to follow the thermal desorption and subsequent readsorption of alkylamines to a $YBa_2Cu_3O_7$ thin film. GRIFTS spectra were taken at each iteration. Initially, a $YBa_2Cu_3O_7$ film was modified with a monolayer of trioctylamine which yielded an IR signature consistent with a disordered monolayer (Figure 7A). The modified film was then annealed in flowing oxygen at 550 °C for 12 h, and the loss of C−H vibrational characteristics were noted (Figure 7B). Immediately after the annealing step and GRIFTS characterization, the film was exposed to a 1 mM solution of octadecylamine to reestablish the monolayer (Figure 7C). From an analysis of the peak

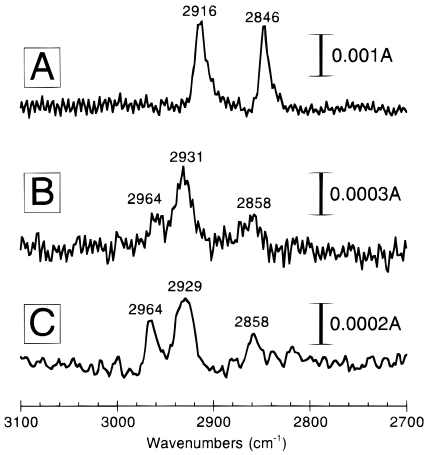

Figure 6. Provided are GRIFTS spectra for three different amine reagents adsorbed to $YBa_2Cu_3O_7$ (001) films. Shown here is data for primary, secondary, and tertiary substituted linear alkylamines: (A) octadecylamine, (B) dioctylamine, and (C) trioctylamine. While the dioctylamine and the trioctylamine samples show disordered or liquid-like behavior, it is apparent that ordered monolayers are obtained with octadecylamine.

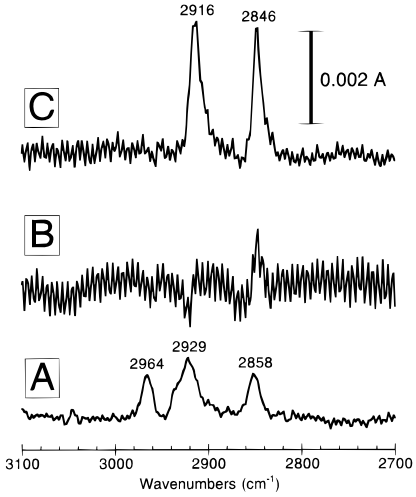

Figure 7. The adsorption and thermal desorption followed by readsorption of various amine reagents atop a single $YBa_2Cu_3O_7$ (001) thin film sample are followed by GRIFTS measurements. (A) Initially, the high-T_c sample is exposed to trioctylamine resulting in the formation of a disordered monolayer. (B) The same sample is subsequently heated to 550 °C in flowing O_2 for 12 h, and the resulting sample shows no infrared signature for adsorbed hydrocarbon. (C) Finally, the same sample was then exposed to octadecylamine and the appearance of an ordered monolayer is observed.

positions, it is clear that the noncrystalline trioctylamine monolayer was removed by the annealing procedure and replaced by the crystalline octadecylamine monolayer. Moreover, it is clear that the surface of the $YBa_2Cu_3O_7$ after monolayer desorption remains receptive to further monolayer adsorption. Thus, thermal desorption appears to be an effective processing procedure that can be exploited to remove the organic layer after its utility is no longer required. This behavior may have important implications in the context of developing "soft chemistry" methods for processing/packaging of high-T_c conductors and devices.

Molecular Modeling. While the above infrared experiments yield essential qualitative information about the ordering characteristics of the amine monolayers on various types of $YBa_2Cu_3O_7$ surfaces, it is desirable to consider in more detail the structural features of the adsorbate layer. Prior successful methodologies for monolayer ordering of the more conventional adsorbate systems such as alkyl thiols on gold (111) have been fully described using popular methods such as ellipsometry and dipolar analysis by polarized infrared data. For the ellipsometric experiments, a number of attempts have been completed and disagreement remains in the literature related to the intrinsic optical constants for $YBa_2Cu_3O_7$.[76] Further work is required here before this technique can be applied to yield reliable information regarding superconductor monolayer structures. Likewise, calculations of molecular tilt angles via the method pioneered by Allara, Chidsey, and Nuzzo[16,18] await more complete characterization of the optical characteristics of $YBa_2Cu_3O_7$ surfaces.

With the advent of powerful computer hardware and efficient software methodologies, computational chemistry is able to provide important structural information for complicated systems.[77,78] Indeed, there is a large body of literature describing computational studies on self-assembled monolayers (SAMs) using molecular mechanics,[79,80] molecular simulations,[81−83] molecular dynamics,[81,84−90] and various other methodologies,[91,92] with the majority of these studies focusing on alkyl thiols adsorbed onto gold (111). Structural information can be obtained through all of these techniques. However, complicated dynamic information on the formation of these monolayers can only be obtained through the more sophisticated techniques, such as molecular dynamics simulations. In this study, our goal is to identify the prominent structural features of the superconductor-localized monolayers. Therefore, we have chosen to employ an efficient molecular mechanics technique for evaluating the favorability of packing arrangements afforded by the permitted degrees of freedom. Although the headgroup−substrate interaction is energetically important for the formation of monolayers, the overall SAM structure is also highly dependent on interchain interactions. The cumulative interactions for the contributing CH_2 groups play an essential role in dictating the structural characteristics of the surface-localized monolayers and is the focus of the modeling studies discussed here. The headgroup−substrate interaction in SAM modeling often serves to keep the chemisorbed molecules in two dimensions and in registry with the substrate.[93] Because this registry is accomplished artificially in our model, the exclusion of the headgroup interaction is not expected to significantly affect the results presented here. More sophisticated molecular dynamic modeling, which incorporates

(76) Gibbons, B. J.; Trolier-McKinstry, S.; Schlom, D. G.; Eom, C. B. *Mater. Res. Soc. Symp.* **1996**, *401*, 333−338.
(77) Davidson, E. R. *Chem. Rev.* **1991**, *91*, 649−1108.
(78) Lipkowitz, K. B.; Boyd, D. B. *Reviews in Computational Chemistry*; VCH: New York, 1990−1997; Vol. 1−10.
(79) Ulman, A.; Eilers, J. E.; Tillman, N. *Langmuir* **1989**, *5*, 1147−1152.
(80) Ulman, A. *Chem. Rev.* **1996**, *96*, 1533−1554.
(81) Shnidman, Y.; Ulman, A.; Eilers, J. E. *Langmuir* **1993**, *9*, 1071−1081.
(82) Siepmann, J. I.; McDonald, I. R. *Langmuir* **1993**, *9*, 2351−2355.
(83) Siepmann, J. I.; McDonald, I. R. *Mol. Phys.* **1992**, *75*, 255−259.
(84) Hautman, J.; Klein, M. L. *J. Chem. Phys.* **1989**, *91*, 4994−5001.
(85) Hautman, J.; Klein, M. L. *J. Chem. Phys.* **1990**, *93*, 7483−7492.
(86) Hautman, J.; Bareman, J. P.; Mar, W.; Klein, M. L. *J. Chem. Soc., Faraday Trans.* **1991**, *87*, 2031−2039.
(87) Bhatia, R.; Garrison, B. *Langmuir* **1997**, *13*, 765−769.
(88) Tupper, K. J.; Brenner, D. W. *Langmuir* **1994**, *10*, 2335−2338.
(89) Tupper, K. J.; Colton, R. J.; Brenner, D. W. *Langmuir* **1994**, *10*, 2041−2043.
(90) Sellers, H.; Ulman, A.; Shnidman, Y.; Eilers, J. E. *J. Am. Chem. Soc.* **1993**, *115*, 9389−9401.
(91) Gerdy, J. J.; Goddard, W. A. I. *J. Am. Chem. Soc.* **1996**, *118*, 3233−3236.
(92) Felix, O.; Hosseini, M. W.; Decian, A.; Fisher, J. *Angew. Chem., Int. Ed. Engl.* **1997**, *36*, 102−104.
(93) Pertsin, A. J.; Grunze, M. *J. Chem. Phys.* **1997**, *106*, 7343−7351.

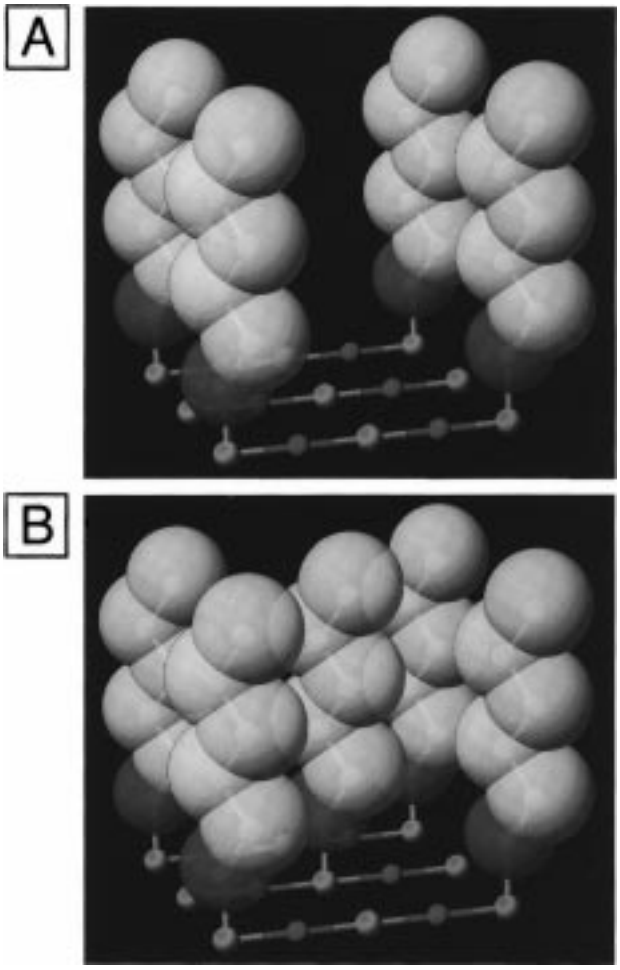

Figure 8. Schematic illustrations showing two clusters of amine reagents adsorbed to a copper oxide table. The amine headgroups are shown in blue, the copper ions in the lattice are shown in green, and the oxygen atoms of the lattice are shown in red. The hydrocarbon layer is shown with 100% van der Waals' radii. Hydrogen atoms are omitted for clarity. The copper oxide "table" in this figure corresponds to the surface of (001) oriented $YBa_2Cu_3O_7$, with the monolayer in a $\sqrt{2}\times\sqrt{2}$R45° adlayer geometry. In case A, four amines at the corners of the table. In case B, the amine located at the center of the table is also included.

the headgroup−substrate interaction, is currently underway and will be the subject of a future report.

To reduce errors associated with edge effects and to create a computationally efficient method to assay the energetic features of the various geometries, two molecular clusters of the type shown in Figure 8 were evaluated. One cluster contains four amine molecules at the corners of a "cuprate table". Note that the middle copper adsorption site is left vacant in this cluster. The second cluster differs by the presence of a fifth amine in the central, previously vacant site. Thus, the amine headgroups are aligned in one plane and spatially separated from one another by a distance corresponding to the $\sqrt{2}\times\sqrt{2}$R45° adlayer separation of (001) oriented $YBa_2Cu_3O_7$.[94] Other arrangements, such as 1×1 or 2×2 adlayers, show less favorable energies.

(94) Energies for 1×1, 2×2, and $\sqrt{2}\times\sqrt{2}$R45° amine adlayers were calculated for various plausible geometries. Here, tables analogous to those described in the text were created to evaluate the energy of amine reagents in environments having all the nearest neighbors present. For the 1×1 case, overlap between neighboring chains precluded any molecular tilt. For the 2×2 case, large separation between sites limited favorable molecular interactions. Comparison of the energies for the various optimized monolayer structures suggests that the $\sqrt{2}\times\sqrt{2}$R45° adlayer is more stable than either the 1×1 or 2×2 arrangements.

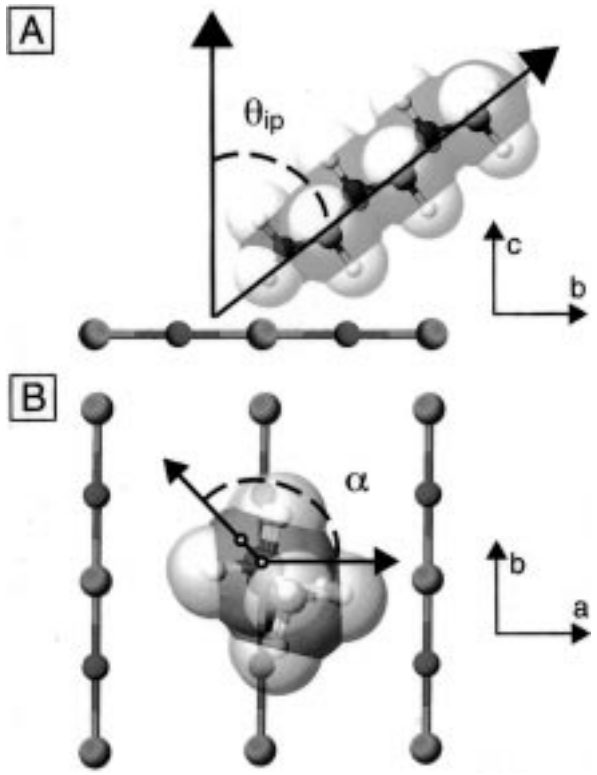

Figure 9. Schematic illustration which details the (A) in-plane tilt (θ_{ip}) and (B) the molecular twist angle (α). For A, θ_{ip} is a measure of the angle between the *c*-axis and the molecular axis projection into the *bc*-plane. The out-of-plane tilt (θ_{op}) is similarly obtained. For B, the twist angle is measured between the plane of the C−C backbone and the *a*-axis of the substrate. The amine headgroups are shown in blue, the copper ions in the lattice are shown in green, and the oxygen atoms of the lattice are shown in red.

The energy of both clusters are evaluated using an MM2 force field. Only the chain interactions are considered; the lattice and headgroup−substrate interaction are not included in these energy calculations. By subtracting the four amine cluster energy from the five amine cluster energy, the contribution for the single amine present with all its nearest neighbors can be obtained. Since the clusters contain a differing number of chains, the intramolecular energy for one chain was removed from the energy difference between the two clusters; only the intermolecular energies were considered. While this model is simple and would not be sufficient for a thorough understanding of the dynamics of monolayer formation, it has the advantages of being a computationally efficient method for evaluating the favorability of packing arrangements afforded by the permitted degrees of freedom.

In this study, three degrees of freedom of molecular orientation were permitted: an in-plane tilt (θ_{ip}), an out-of-plane tilt (θ_{op}), and a twist (α) around the molecular axis of each molecule. A schematic illustrating two of these degrees of freedom is shown in Figure 9. Here, the amine chain orientation will be described in terms of local $YBa_2Cu_3O_7$ lattice parameters. The amine nitrogens are coplanar in the *ab*-plane (substrate plane). Tilt angles were measured using the angle formed by the molecular axis, as defined by the line bisecting the first and last carbon−carbon bonds on the chain, and the *c*-axis (surface normal). The in-plane tilt (θ_{ip}) is defined as the angle between the projection of the molecular axis into the *bc*-plane and the *c*-axis of the lattice. Similarly, the out-of-plane tilt (θ_{op}) is defined as the angle between the projection of the molecular axis into the *ac*-plane and the *c*-axis of the cuprate lattice. The

twist angle is defined as the angle formed by the *b*-axis and the projection from the middle methylene carbon (i.e., the γ carbon to the amine headgroup) through the midpoint of its two hydrogens onto the *ab*-plane. Here, a zero degree twist angle ($\alpha = 0°$) is defined as the projection lying in the *bc*-plane (i.e., along the positive *b*-axis).

Since spectroscopic evidence indicates that the adsorbed monolayer is crystalline, it is reasonable to assume that the chemical homogeneity of the system is relatively high. Therefore, all of the alkyl chains in the clusters are treated as being identical in conformation and orientation relative to the underlying lattice. Also, the favored molecular conformation in the monolayer and the molecular conformation for an isolated molecule are not expected to differ significantly, because of the simplicity of the rodlike molecular shape and the dominance of van der Waals' interactions among the chains.[95] Thus, exact duplicates of a chain which was *ab initio* optimized as an isolated molecule were used to construct the modeled patterns. Once the molecules were in the modeled pattern, the molecules were not permitted to change their intramolecular geometry characteristics.

To justify the use of an MM2 force field in these computations, we carried out identical MNDO-PM3 and MM2 studies on a representative system. Specifically, we examined the energy difference between the five- and four-amine clusters as a function of the in-plane tilt. The results indicated that both the MNDO-PM3 model and the less-sophisticated MM2 model predict a 53° in-plane angle for the representative system. Moreover, the curves are virtually identical in magnitude of energy difference and functional shape.

The above-described procedure possesses an advantage over some prior studies on other SAM systems in which clusters were used with incomplete nearest neighbor arrangements. For example, a linear patch of three alkyl thiols spaced at the gold (111) separation distance was found to exhibit an optimal tilt angle of 32°.[96] When our cluster arrangement and computational procedure is applied to the alkyl thiol case to extract the energy for a single thiol with its six nearest neighbors, we find the largest energy difference between the two clusters and, thus, the best packing arrangement occurs with an alkyl thiol molecular tilt of 29° away from the gold surface normal along with twist about the molecular axis of 63° (Figure S5, Supporting Information). These values agree nicely with the experimentally reported values of molecular tilt and twist angles of 27° and 55°, respectively,[51] and provide credence to the described computational method. Thus, the use of the complete set of nearest neighbors combined with the identification of the energetic characteristics of single adsorbate reagents appears to be an effective procedure for the modeling of ordered adsorbate layers systems.

Although Kitaigorodoskii did extensive studies on the possible forms of packing of infinite hydrocarbon chains,[97] the degree to which monolayer tilting influences the energy for orthorhombic $YBa_2Cu_3O_7$ supported monolayers has yet to be reported. Therefore, the energy of a series of clusters having different combinations of the two tilt angles and twist angle were investigated. To reduce the amount of computational time required to complete this study, logical assumptions were made and tilt angle combinations that would clearly not yield minimum energies were discarded. Also in the interests of reduced computational time, five-carbon amine chains were used to search for plausible structures. However, strategically important areas were also evaluated using 10-carbon-chain amines; all of the optimal angles obtained with these longer chains agreed nicely ($\pm 1°$) with the shorter chain results. A series of two-dimensional slices through the three-dimensional energy difference surface are presented here.

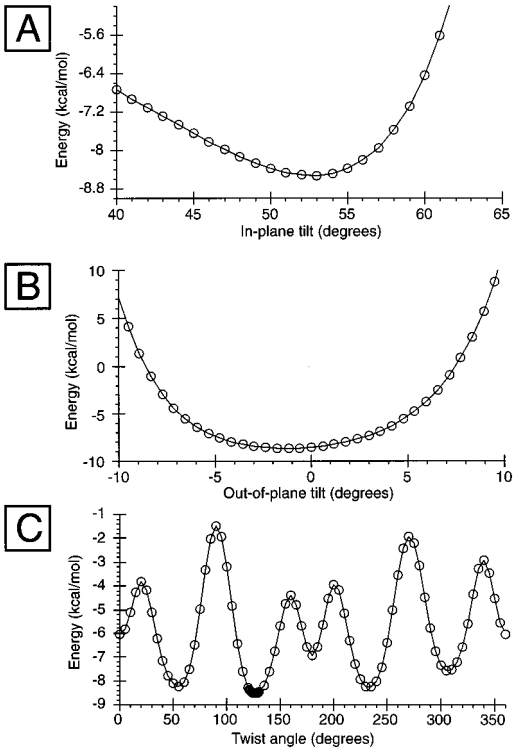

Figure 10. Energy characteristics of uniformly organized adsorbate layers having various structures. A multidimensional energy contour map is created where values of θ_{ip} (A), θ_{op} (B), and α (C) are varied. Two-dimensional slices are obtained through the energy surface near the energy minimum which focus on curves associated with lowest identified energy minimum, $\theta_{ip} = 53°$, $\theta_{op} = 0°$, and $\alpha = 126°$. Three curves are provided: (A) energy vs θ_{ip} where fixed values of $\theta_{op} = 0°$ and $\alpha = 126°$ are used, (B) energy vs θ_{op} where $\theta_{ip} = 53°$ and $\alpha = 126°$, and (C) energy vs α where $\theta_{ip} = 53°$ and $\theta_{op} = 0°$ are used.

Two plausible monolayer geometries corresponding to two minima located on the energy difference surface were identified. The deepest minimum occurs at $\theta_{ip} = 53°$, $\theta_{op} = 0°$, and $\alpha = 126°$. The graphs of energy differences as a function of these variables are shown in Figure 10. Space-filling diagrams of the five-amine cluster of this best packing geometry is shown in Figure 11A,B. It is apparent from careful inspection of the optimized geometry that excellent van der Waals' contacts occur in this system by interdigitation of the hydrogens with the central amine (Figure 11B). The large in-plane tilt in this geometry precludes any significant out-of-plane tilting of the amine reagents toward the diagonal direction of the lattice (i.e., along the 110 plane). With this geometry, the molecular tilt occurs in a direction which coincides nicely with the *b*-axis direction of the high-T_c substrate. Note that in this direction, the amine reagents seek out the association with their next nearest neighbors. Tilting along the principal axis directions allows for this large value for the molecular tilt axis.

Careful evaluation of the energetic characteristics of alternative geometries reveals a second minimized structure occurring at $\theta_{ip} = 32°$, $\theta_{op} = 14°$, and $\alpha = 120°$ (Figure S6, Supporting Information). This favorable five-amine cluster is shown in

(95) Nuzzo, R. G.; Korenic, E. M.; Dubois, L. H. *J. Chem. Phys.* **1990**, *93*, 767−775.

(96) Ulman, A.; Eilers, J. E.; Tillman, N. *Langmuir* **1989**, *5*, 1147−1152.

(97) Kitaigorodskii, A. I. *Organic Chemical Crystallography*; Consultants Bureau Enterprises, Inc.: New York, 1961.

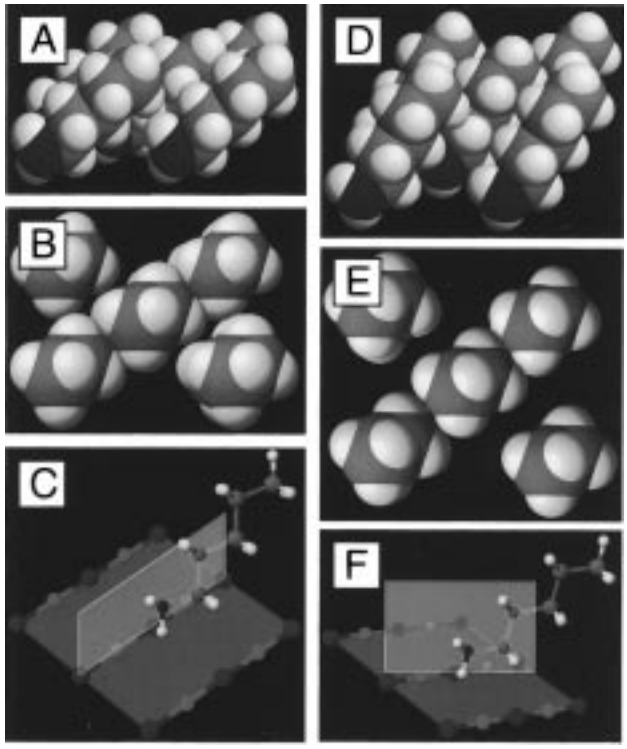

Figure 11. Molecular models showing the packing and orientational properties of the lowest energy system: $\theta_{ip} = 53°$, $\theta_{op} = 0°$, and $\alpha = 126°$. Included are three different views: (A) side perspective of the space filling structure, (B) similar structure viewed from the top surface down the molecular axis, and (C) a single adsorbate molecule is isolated and shown with respect to the crystallographic axes of the $YBa_2Cu_3O_7$ (001) superconductor substrate. Shown in (D), (E), and (F) are analogous views for the minimum encountered at $\theta_{ip} = 32°$, $\theta_{op} = 14°$, and $\alpha = 120°$.

Figure 11D,E,F. Again, the interdigitation of the hydrogens with the central amine provides good van der Waals' contacts. By viewing down the molecular axes of these clusters (Figure 11B,E), the superiority of the 53°, 0°, 126° geometry's packing can be seen; the gaps between the chains in this geometry are much smaller than the 32°, 14°, 120° geometry.

As expected for a rectangular substrate system, the twist angle (α) in both geometries exhibits a 4-fold periodicity. The twist angle plays a significant role in both geometries, exhibiting a calculated barrier to rotation of about 1.5 kcal mol^{-1} per methylene unit in the 53°, 0°, 126° case. For comparison, using the same computational method, the barrier to rotation found for the alkyl thiol/gold system is about 1.8 kcal mol^{-1}. The high-energy twist angle geometries result from extremely close chain contacts. Because of the rigidity found in the alkyl thiol/gold (111) system[98] and the similarity of rotational energy barriers between the two systems, we expect that there will be little rotation about the molecular axes for the superconductor-localized reagents. The barrier to rotation is lowered in the 32°, 14°, 120° case as the amines have more space available before encountering their neighbor. However, the barrier is still significant for this geometry. It is important to note that the absolute values of the calculated energies are not meant to provide an accurate measure of the energetic characteristics of real systems. Rather, meaningful comparisons are made with respect to the relative calculated values.

While these minima appear significant in our assay of the energy difference surface, certain precautions must be heeded when evaluating these results. As mentioned previously, this model can neither account for the dynamics of monolayer formation nor include interactions with the substrate. Thus, the tilt and twist angles described here are representative of the best packing as influenced by chain interaction for the prescribed spacing. More sophisticated molecular dynamics calculations involving this interaction are underway. Also, these two minima are not the only ones on the energy difference surface. Because the lattice constants for the *a*- and *b*-axes are similar for $YBa_2Cu_3O_7$, we expect that the minima at both these geometries have "mirror" minima, i.e., $\theta_{ip} = 0°$, $\theta_{op} = 53°$, $\alpha = 126°$ would be close to another minimum. Furthermore, the energy differences between the $\theta_{ip} = 53°$, $\theta_{op} = 0°$, and $\alpha = 126°$ and $\theta_{ip} = 32°$, $\theta_{op} = 14°$, and $\alpha = 120°$ geometries are modest. Thus, it is likely that both structural types can exist simultaneously atop real samples of $YBa_2Cu_3O_7$ (001) which are modified with long alkyl chain primary amine reagents.

Importantly, the rather large tilt angles predicted by these computational studies are consistent with experimental evidence. To couple to the incident radiation in a GRIFTS experiment, it is necessary to have a component of the vibrational dipole that is perpendicular to the substrate. Assuming that the monolayer assumes a tilt angle of 53°, the dipole of the methyl symmetric stretching mode lies at an angle of 87° away from the substrate normal (Figure S2, Supporting Information). The dipole projection is nearly parallel to the substrate surface where coupling to the incident radiation is expected to be very weak. In addition, the vibrational dipole of the out-of-plane asymmetric methyl stretch lies in the plane of the substrate. The vibrational dipole of the in-plane asymmetric methyl stretch has a component that lies perpendicular to the substrate. Interestingly, this mode has not been identified in the $YBa_2Cu_3O_7$/alkylamine system when adsorbed to (001) oriented $YBa_2Cu_3O_7$. This mode is also not observed in the alkyl thiol/GaAs (100) system.[27] Allara and co-workers ascribed the high tilt angle of this system as being responsible for the low signal from this vibration. The large tilt angle predicted by computer modeling of the $YBa_2Cu_3O_7$/alkylamine system combined with the low absorbance value observed for the one methyl group per adsorbate molecule adequately explains the observed low signal intensity for this vibration.

Summary

New procedures have been developed for the preparation and analysis of superconductor-localized monolayers structures. Here, the following important information has been acquired: (1) GRIFTS methods have been successfully employed for the first time to evaluate the structural characteristics of cuprate monolayers. Such measurements have become possible only following the identification of important experimental variables such as superconductor sample thickness, substrate roughness, and monolayer formation procedures. (2) Likewise, a large substrate orientation dependence is noted for this system. Oriented films of $YBa_2Cu_3O_7$ (001) are shown to support crystalline-like monolayers, while polycrystalline samples yield disordered adsorbate layers. (3) Furthermore, a substitution pattern dependence for amine reagents is observed. Primary amines form crystalline monolayers, while secondary and tertiary amines form disordered monolayers on $YBa_2Cu_3O_7$ (001). (4) A plausible adsorbate layer structure of $\sqrt{2}\times\sqrt{2}R45°$ has been proposed, and calculations examining alkylamine packing support this adsorbate layer structure as the favored one for long linear chain reagents. (5) An efficient and simple computational method has been devised for the evaluation of

(98) Karpovich, D. S.; Blanchard, G. J. *Langmuir* **1996**, *12*, 5522−5524.

the energies of adsorbate layer structures. Although this new method does not incorporate the headgroup−substrate interaction, it has been tested on the well studied alkyl thiol/gold (111) system and found to yield results which agree extremely well with the accepted experimental values. The method has been applied also to the alkylamine/$YBa_2Cu_3O_7$ (001) adsorbate structure where two distinct, stable structures have been identified. The most energetically stable system found from the computational experiments would be expected to yield reflectance IR characteristics consistent with the observed experimental data. (6) Methods for the thermal desorption of the amine reagents from the high-T_c surface have been developed as have strategies for the subsequent readsorption of similar reagents. The reversible adsorption/desorption process noted here suggest that the described "soft chemistry" procedures may be effective for the molecular-level control of superconductor interfacial properties.

Acknowledgment. J.T.M. and D.R.K. acknowledge the Air Force Office of Scientific Research and the National Science Foundation for support of this work. J.T.M. acknowledges the Office of Naval Research for support of this work. J.E.R. acknowledges the support of a University of Texas Continuing Fellowship. D.R.K. acknowledges the Camille and Henry Dreyfus Foundation for support of this work. Professors Al Bard and James Whitesell are thanked for use of their instrumentation. Professors David Allara and Chad Mirkin, and Dr. Atul Parik are thanked for useful discussions.

Supporting Information Available: Supplementary Figures S1−S6 (8 pages). See any current masthead page for ordering information and Web access instructions.

Note Added in Proof. From our studies of a variety of hydrocarbon amine and fluorocarbon amine reagents by X-ray photoelectron spectroscopy, we have obtained important information regarding the nature of the adsorbate−surface headgroup interaction. Likewise, convincing evidence has now been obtained which suggests a strong interaction occurs between the amine lone pair and the copper ions from the high-T_c lattice. A more detailed description of this work will soon be published elsewhere (J. E. Ritchie, J. T. McDevitt, manuscript in preparation). This new information provides the direct experimental evidence which defines the location of the adsorbate docking site and supports the adsorbate−surface binding mode hypothesized in this manuscript.

JA9706920